MGS-TES Spectra of Phobos Indicate Thermally Homogeneous Surface N. M. Smith[1], C. S. Edwards[1], M. Mommert[2], D. E. Trilling[1], T. D. Glotch[3], [1]Department of Physics and Astronomy, Northern Arizona University, Flagstaff, AZ, 86011, Nathan.Smith@nau.edu, [2]Lowell Observatory, Flagstaff, AZ, 86001, [3]Department of Geosciences, Stony Brook University, Stony Brook, NY, 11794

Introduction. The moons of Mars are the only other moons—beside our own—that orbit a terrestrial planet. They may have an origin as captured carbonaceous asteroids [1], or as accreted or re-accreted ejecta originating from a giant impact [2, 3]. Mars-observing spacecraft have had the opportunity to study Phobos from Mars orbit (e.g. Mars Reconnaissance Orbiter (MRO), 2001 Mars Odyssey, Mars Express (MEx), Viking Orbiters) and as they enter low orbit (e.g. Mars Global Surveyor (MGS)). These missions have produced a long record of observations of Phobos using the same instruments that were designed to study the surface of the planet below. These observations, however, are generally few and far between [4], and are acquired rarely over each mission.

Close (i.e., resolved) observations of Phobos by spacecraft began in 1971 with the first visible light imaging and two-channel infrared radiometry [5]. Infrared observations continued with the Viking orbiters in 1976 [6], and the Phobos 2 mission in 1989 [7]. MGS's Phobos encounters in 1997 are described below. Since MGS, MRO (beginning 2006), MEx (beginning 2003), and Mars Odyssey (beginning in late 2017) have each recorded spectra of Phobos as they occasionally have opportunities in their orbits. [8,9] These observations have resulted in compositional information of Phobos's surface [10-12].

Using these observations, we can begin to characterize this surface, which is likely blanketed in a layer of fine regolith [5]. The properties of this regolith determine how heat is absorbed, transferred, and re-radiated to space. We use thermophysical modeling to simulate these processes and predict, for a given set of assumptions and parameters, the observed thermal infrared spectra. By comparing models to observations, we can constrain the properties of the regolith, such as thermal inertia (how well heat is retained in the surface over time) and surface roughness. With many observations, we can also begin to understand how these properties vary regionally across the surface. These constraints are key to understanding how Phobos formed and evolved over time, which in turn informs us about the environment and processes that shaped the Martian system, and the solar system as a whole.

Thermophysical Model. We have developed a thermophysical model of Phobos adapted from a model used for unresolved observations of asteroids [13]. Our Phobos model uses the complete 3D shape model [14] to define the facets that make up the modeled surface, improving on prior thermal models which used a tri-axial ellipsoid approximation.

Several significant modifications were made to adapt the asteroid model for use with Phobos. Unlike sun-orbiting asteroids, Phobos receives significant scattered, reflected, and thermal radiation from the Martian surface. Phobos is also eclipsed by Mars. Another significant change is the linking of the model to resolved observations from Mars-orbiting spacecraft. As the model had previously been used for unresolved observations only, the model had to be restricted to simulate only the facets observed by MGS's Thermal Emission Spectrometer (TES) [15]. By only simulating the region within each TES field of view, the simulated spectra corresponded to the flux integrated across the portion of the Phobos surface where each observation was made.

Thermal Infrared Spacecraft Observations. The mapping of TES field of view footprints to the Phobos surface took into account spacecraft orientation, TES pointing mirror angle and the positions of both MGS and Phobos (using SPICE) [12]. Over 350 resolved observations of Phobos are available from three orbits (under TES' Orbit Counter Keeper numbering [15], these were OCKs 501, 526, 551). These provide ~50% coverage of the Phobos surface.

A subset of observations fell within local times during the evening thermal cross-over period, when many combinations of thermal inertia and surface roughness produce identical surface temperatures. We selected only observations during overnight local times (1900-0400 LST), when thermal inertia most strongly determines temperature. As all three OCKs' observations were made at similar times in Phobos' orbit, this local time selection restricted our study area to Phobos' eastern hemisphere.

Each observation was mapped to a set of facets in the Phobos shape model that fell within the field of view of one of TES's six detectors. While far from complete coverage, these data, when combined with the newly adapted thermal model, provide insights into the variations of thermophysical parameters across the surface.

As we are primarily concerned with the thermal properties of the surface, rather than composition, each

TES spectrum was converted from radiance to brightness temperature [15].

Comparison of Model and Observations. The geometry of each observation (i.e., the position and orientation of the Sun, Mars, Phobos, and MGS) was extracted using SPICE, and input into the model, along with the facets included in the observation footprint. The model then generated a corresponding scenario and returned the flux received by the simulated detector at a series of wavelengths. The scenario was remodeled inputting six different assumed thermal inertias (10, 25, 50, 85, 130, and 250 J m^{-2} K^{-1} $s^{-½}$). The resulting infrared fluxes were converted to brightness temperatures at the set wavelengths. Fig. 1 shows a comparison between the modeled and observed brightness temperatures.

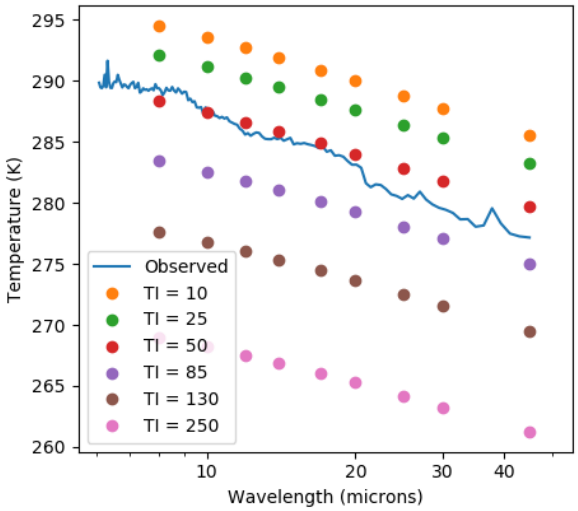

Figure 1. Comparison of brightness temperatures observed by TES (line), and produced by model (points) assuming various thermal inertias, for one observation footprint. Varying surface roughness did not visibly alter these results.

These temperatures were then interpolated to find the thermal inertia corresponding to the observed temperature for that observation. In this way, we derived a thermal inertia for each observation.

Results and Discussion. Using 10 μm measurements, we derive an average thermal inertia of 42 ± 14 J m^{-2} K^{-1} $s^{-1/2}$ for the observed region, with local variations ranging from ~20 – 70 J m^{-2} K^{-1} $s^{-1/2}$. This is similar to the ~50 J m^{-2} K^{-1} $s^{-1/2}$ thermal inertia of lunar regolith, composed primarily of fine dust [16]. Our result is consistent with prior estimates of Phobos' global average thermal inertia, which ranged from ~40-70 J m^{-2} K^{-1} $s^{-½}$ [6] to ~80-170 J m^{-2} K^{-1} $s^{-½}$ [17].

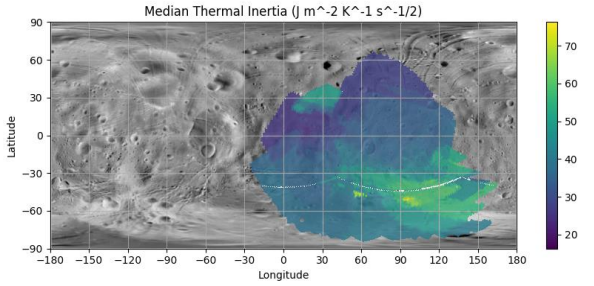

Figure 2. Thermal inertia of Phobos, in units of J m^{-2} $K^{-1}s^{-1/2}$. Thermal inertia varies by only a small degree, suggesting a relatively homogeneous surface.

As Fig. 2 shows, the variation in thermal inertia across the observed hemisphere is fairly small, only a few 10s of J m^{-2} K^{-1} $s^{-½}$. No provinces of anomalously high thermal inertia material appear to exist, at least not at the resolution of our observations.

References: [1] Pang K. D. et al. (1978) *Science, 199*, 64-66. [2] Hyodo R. et al. (2017) *ApJ, 845*, 125. [3] Hesselbrock A. J. and Minton, D. A. (2017) *Nature Geoscience, 10*, 266-269. [4] Duxbury T. C. et al. (2014) *Planet. Space Sci., 102*, 9-17. [5] Gatley I. et al. (1974) *ApJ, 190*, 497-508. [6] Lunine J. I. et al. (1982) *JGR: Solid Earth, 87*, 10297-10305. [7] Bibring J. P. et al. (1989) *Nature, 341*, 591-593. [8] Murchie S. L. et al. (2008) *LPS XXXIX*, Abstract #1434. [9] Witasse O. et al. (2014) *Planet. Space Sci., 102*, 18-34. [10] Giuranna M. et al. (2011) *Planet. Space Sci., 59*, 1308-1325. [11] Fraeman A. A. (2014) *Icarus, 229*, 196-205. [12] Glotch T. D. et al (2018) *JGR: Planets, 123*, 2467-2484. [13] Mommert M. et al. (2014) *ApJ, 786*, 148. [14] Gaskell R. W. (2011) *NASA PDS, 154*. [15] Christensen P. R. et al. (2001) *JGR: Planets, 106*, 23823-23871. [16] Hayne P. O. et al (2017) *JGR: Planets, 122*, 2371-2400. [17] Ksanfomality, L. V. et al. (1989) *Nature, 341*, 588-591.